

UDC 539.3

## FIRST BASIC PROBLEM OF ELASTICITY THEORY FOR A COMPOSITE LAYER WITH TWO THICK-WALLED TUBES

**Oleksandr Yu. Denshchykov**

[Alex\\_day@ukr.net](mailto:Alex_day@ukr.net)

ORCID: 0009-0008-2385-5841

**Valentyn P. Pelykh**

[venator.verba@gmail.com](mailto:venator.verba@gmail.com)

ORCID: 0009-0007-5301-6697

**Yaroslav V. Hrebenuk**

[i.grebenuk@khai.edu](mailto:i.grebenuk@khai.edu)

ORCID: 0009-0004-6032-7125

**Vitalii Yu. Miroshnikov**

[v.miroshnikov@khai.edu](mailto:v.miroshnikov@khai.edu)

ORCID: 0000-0002-9491-0181

National Aerospace University

"Kharkiv Aviation Institute"

17, Vadyma Manka str., Kharkiv,

61070, Ukraine

### Introduction

Fibrous composites are often used in mechanical and aircraft engineering, which increases the requirements for assessing the stress-strain state of such bodies and forces us to search for the most effective calculation methods. The model of fibrous composites is represented as an infinite layer with longitudinal inclusions. The cross-sections of the inclusions can be of various shapes, solid or with cavities. In addition, various boundary conditions can be set on the surfaces of the model, in particular, the conjugation surfaces.

The embedded tube layer model is used in: cooling systems (in engines and other mechanisms, tubes can be embedded in layers of structures to circulate coolant), fuel systems (in some structures, tubes can be embedded in metal layers to transport fuel to engines or other machine components), for noise absorption and vibration isolation (in tubes embedded in layers of structures, air or other gases can circulate, which helps reduce vibrations or noise in mechanical systems), in turbochargers (in turbines and compressors, tubes can be embedded in layers of the housing to supply air or gas under pressure to turbo-supercharging systems), in lubrication systems (in mechanical engineering, tubes embedded in layers of metal structures can provide lubrication to critical parts of machines and mechanisms, reducing friction and wear).

One of the approaches to solving problems with composites is testing samples from finished sheets [1]. In this case, the reinforced layer is represented as a physically nonlinear material with anisotropic characteristics. This is well suited for a stochastic structure or for a layer with a large amount of reinforcement [2]. However, this approach significantly complicates the design with variable geometric characteristics of the composite or variable boundary conditions. Taking the above into account, in most papers the composite is considered as a set of conjugated elements. In view of this, when solving problems with composites, analytical, analytical-numerical or numerical methods are used, sometimes these methods are combined with each other and with tests.

*The spatial problem of elasticity theory for a fibrous composite in the form of a layer with two thick-walled cylindrical tubes is solved. Stresses are given on the flat surfaces of the layer and on the inner surface of the tubes. The solution to the problem is presented in the form of Lamé equations in different coordinate systems, where the layer is considered in a Cartesian system and the tubes – in local cylindrical ones. To combine the basic solutions in different coordinate systems, the generalized Fourier method is used. Satisfying the boundary conditions and conjugation conditions between the layer and the tubes, an infinite system of integro-algebraic equations is formed, which is reduced to linear algebraic equations of the second kind, and the reduction method is applied. After finding the unknowns, it is possible to obtain the stress-strain state at any point of the elastic combined bodies using the generalized Fourier method to the basic solutions of the problem. According to the results of numerical studies, it can be stated that the problem can be solved with a given accuracy, which depends on the order of the system of equations and has a rapid convergence of solutions to the exact one. Numerical analysis of the stressed state was considered with a variation of the distance between the tubes. The graphs of the distribution of internal stresses in the tubes and the layer are obtained. The results show an inverse relationship between the magnitude of stresses and the distance between the tubes. In addition to the absolute value of stresses, changes in the character of the diagrams and the sign are possible. The proposed method of solution can be applied in the design of a layer with tubes. The obtained stress-strain state makes it possible to preliminarily evaluate the geometric parameters of the structure. Further development of the research topic is necessary for a model where tubes are combined with other types of inhomogeneities.*

**Keywords:** fibrous composite, generalized Fourier method, Lamé equation.

This work is licensed under a Creative Commons Attribution 4.0 International License.

© Oleksandr Yu. Denshchykov, Valentyn P. Pelykh, Yaroslav V. Hrebenuk, Vitalii Yu. Miroshnikov, 2024

As experience shows, most often when solving such problems, numerical methods [3] and computer programs based on them [4] are useful. Thus, in paper [5], the finite element method was applied to the problem for a half-space reinforced with a shell and a vertical cylindrical cavity. However, numerical methods give approximate values of the stress-strain state, which does not add confidence when a highly accurate result is required. This forces us to look for other methods or additional approaches.

Classical analytical methods [6, 7] are considered accurate. They are based on the Fourier series expansion of solutions. However, classical methods do not allow to solve spatial problems when the model contains more than three boundary surfaces, which is typical for composites.

There are a number of papers [8–11], which consider problems for composites taking into account the nonlinearity of the model.

Thus, in the study [8], the problem of determining the dynamic stress state for two rods of different lengths connected in an overlap, and with a longitudinal load applied to one of the rods, was solved. The Holland-Reisner model was used to model the adhesive joint, in which the support layers are considered as beams in the Bernoulli approximation, and the adhesive layer is considered as an elastic Winkler base.

In [9], a multilayer structure under the action of dynamic transverse loading was analyzed. The solution consisted in using a two-dimensional discrete structure, and the displacement vector was expanded into a power series. The solution is correlated with the results of an experimental study.

In the paper [10], a method for calculating the thermo-stressed state of an aircraft double-glazed window was proposed. In this case, the double-glazed window was considered as a cylindrical laminated open shell of constant thickness under the action of convection heat transfer. Similarly to the previous study, the results correspond to the experimental data.

In [11], a method for analyzing the stress-strain state of a laminated composite during a collision with a bird and the action of internal excess pressure was presented. The model of a laminated double-glazed window is based on a theory that takes into account transverse shear deformations, thickness reduction and inertial phenomena. The mathematical pressure model that reproduces the bird strike is based on experimental studies.

At the same time, the methods used in [8–11] do not allow for cylindrical cavities or inclusions to be taken into account.

In [12–17], cylindrical inhomogeneities located perpendicular to the layer boundaries are considered.

Thus, in [12], the problem is solved by assuming ideal contact conditions at the upper and lower boundaries of the layer. In [13], a similar approach is used, but on the condition that the lower surface of the layer is rigidly clamped. The problem of a layer with a cylindrical inclusion or cavity running parallel to the layer boundaries cannot be solved by the methods proposed in these papers, since the use of integral Laplace transforms and integral sine and cosine Fourier transforms to the boundary conditions and equations of motion creates a one-dimensional vector inhomogeneous boundary value problem that can provide solutions only for wave diffraction problems.

For a perforated plate, stress analysis using the genetic algorithm (GA), gravity search algorithm (GSA) and Bat algorithm (BA) was applied in [14], but the proposed approach is also approximate.

In [15], the torsion of an elastic half-space with a vertical cylindrical cavity and a coaxial die was considered. The problem was solved by two innovative methods that reduced the solution to ordinary integral equations of the second kind. At the same time, the solution is quite approximate and has some discrepancies with the solution of the Reisner-Sagoci problem.

In [16], an analytical solution based on the layer-beating method was developed for composite laminated perforated plates. The reliability and accuracy of the proposed method were confirmed by comparison with finite element calculation. In [17], the problem of torsional vibrations of a flat circular die conjugated to the upper boundary of a multilayer elastic base containing a vertical cylindrical cavity with an axis perpendicular to the boundary of the layers was solved. The Weber integral transformation and pair integral equations are used for the solution. The methods discussed in the studies [16, 17] are not suitable for solving problems with inhomogeneities located parallel to the layer.

The aim of this paper is to create a high-precision method for solving the problem of the theory of elasticity for a layer with two longitudinal cylindrical thick-walled pipes. The stresses are given on the surfaces of the layer and on the inner surfaces of the pipes. The layer and pipes are rigidly conjugated.

The most effective method that allows to obtain accurate results of the specified model is the analytical-numerical generalized Fourier method [18]. Its main advantage is that it allows to obtain a solution for a group of bodies, each of which has its own coordinate system. At the same time, using the transition functions between the basic solutions of the Lamé equation, it is possible to apply different types of coordinate systems simultaneously.

Using the generalized Fourier method, solutions were obtained for an elastic cylinder with cylindrical cavities [19, 20] and cylindrical inclusions [21], as well as for a half-space with a spheroidal cavity [22]. The solution is presented as a superposition of the exact basic solutions of the Lamé equation for a cylinder in coordinate systems referred to the centers of the boundary surfaces of the body.

A further development of the method is the application of the formulas for the transition of the basic solutions between the cylindrical and Cartesian coordinate systems. The following developments can be an example: in [23] such formulas are proposed for a half-space with a cylindrical cavity, in [24] – for a layer with a cavity on the surface of which stresses are given, in [25] a solution for a layer with a cylindrical inclusion is shown. However, a general drawback of the papers [23–25] is the presence of only two independent coordinate systems: Cartesian for a layer or half-space and cylindrical for inhomogeneity. In this case, the formulas for the transition between local cylindrical coordinate systems are not used, which does not allow to solve a problem with several inhomogeneities.

The increase in the number of bodies taken into account in the calculation model is discussed in [26–28]. Moreover, in [26], the situation is considered when Cartesian coordinate systems are used for two bodies (layer and half-space), and cylindrical coordinate systems are used for inhomogeneity. Problems in which the layer is fixed on two supports are solved in [27], and for a layer with two cylindrical inclusions having mixed boundary conditions – in [28]. However, the approach used in [26–28] does not allow for inclusions in the form of thick-walled pipes to be taken into account. The approach that takes thick-walled pipes into account is implemented in [29, 30], where a layer with one thick-walled pipe is considered. This approach, as mentioned above, allows for more accurate modeling of the support itself and the conditions of attachment to it, but the disadvantage of these papers is, as for papers [23–25], the lack of formulas for transition between cylindrical coordinate systems in which the origin points do not coincide. The application of such formulas and consideration of problems where supports are modeled in the form of several pipes is the subject of this study.

**Problem statement**

The model is a composite in the form of an elastic layer with two cylindrical thick-walled pipes located parallel to its boundaries (Fig. 1).

The boundary conditions are presented in the form of stresses on the flat surfaces of the layer and the inner surfaces of the pipes. The outer radii of the pipes are indicated by  $R_p$ , and internal ones – by  $\tilde{R}_p$ , where  $p$  – pipe number. The layer was considered in the Cartesian coordinate system  $(x, y, z)$ , pipes – in local cylindrical coordinate systems  $(\rho_p, \varphi_p, z)$ . Distance to layer boundaries:  $y=h$  and  $y=-\tilde{h}$ .

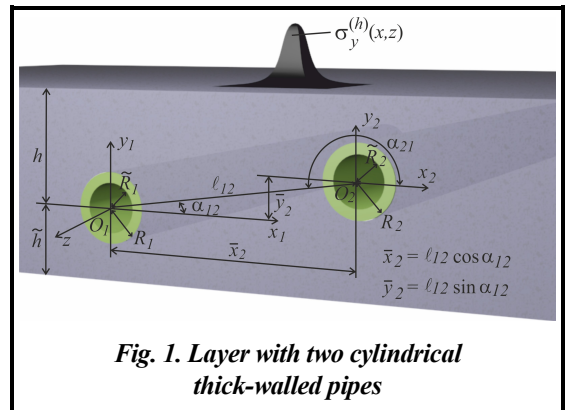


**Fig. 1. Layer with two cylindrical thick-walled pipes**

To solve the problem, it is necessary to find a solution to the Lamé equations in the form

$$\Delta \bar{u} + (1 - 2\sigma)^{-1} \nabla \operatorname{div} \bar{u} = 0.$$

The stresses are given at the upper and lower boundaries of the layer, as well as on the inner surfaces of the pipes  $F\bar{U}(x, z)|_{y=h} = \bar{F}_h^0(x, z)$ ,  $F\bar{U}(x, z)|_{y=-\tilde{h}} = \bar{F}_{\tilde{h}}^0(x, z)$ ,  $F\bar{U}(\rho_p, z)|_{\rho_p=R_p} = F\bar{U}_0^{(p)}(\rho_p, z)$  respectively,

where  $\bar{U}$  is the displacement in a layer;  $F\bar{U} = 2 \cdot G \cdot \left[ \frac{\sigma}{1 - 2 \cdot \sigma} \bar{n} \cdot \operatorname{div} \bar{U} + \frac{\partial}{\partial n} \bar{U} + \frac{1}{2} (\bar{n} \times \operatorname{rot} \bar{U}) \right]$  is the stress operator;

$$\begin{aligned} \bar{F}_h^0(x, z) &= \tau_{yx}^{(h)} \bar{e}_x + \sigma_y^{(h)} \bar{e}_y + \tau_{yz}^{(h)} \bar{e}_z, \\ \bar{F}_{\tilde{h}}^0(x, z) &= \tau_{yx}^{(\tilde{h})} \bar{e}_x + \sigma_y^{(\tilde{h})} \bar{e}_y + \tau_{yz}^{(\tilde{h})} \bar{e}_z, \quad - \text{known functions.} \\ F\bar{U}_0^{(p)}(\rho_p, z) &= \sigma_\rho^{(p)} \bar{e}_\rho + \tau_{\rho\varphi}^{(p)} \bar{e}_\varphi + \tau_{\rho z}^{(p)} \bar{e}_z \end{aligned} \tag{1}$$

The layer is rigidly connected to each pipe where the conjugation conditions are met

$$\vec{U}_0(\varphi, z)|_{\rho=R_p} = \vec{U}_p(\varphi, z)|_{\rho=R_p}, \quad (2)$$

$$F\vec{U}_0(\varphi, z)|_{\rho=R_p} = F\vec{U}_p(\varphi, z)|_{\rho=R_p}, \quad (3)$$

where  $\vec{U}_0(\varphi, z)$  is the solution for the layer;  $\vec{U}_p(\varphi, z)$  is the solution for the pipes.

All given functions will be considered to be rapidly decreasing from the origin along the axis  $z$  and axis  $x$ .

### Solution method

When solving the problem, the displacement in the layer was represented in the form proposed in the paper [28]

$$\begin{aligned} \vec{U}_0 = & \sum_{p=1}^2 \sum_{k=1}^3 \int_{-\infty}^{\infty} \sum_{m=-\infty}^{\infty} B_{k,m}^{(p)}(\lambda) \cdot \vec{S}_{k,m}(\rho_p, \varphi_p, z; \lambda) d\lambda + \\ & + \sum_{k=1}^3 \int_{-\infty}^{\infty} \int_{-\infty}^{\infty} (H_k(\lambda, \mu) \cdot \vec{u}_k^{(+)}(x, y, z; \lambda, \mu) + \tilde{H}_k(\lambda, \mu) \cdot \vec{u}_k^{(-)}(x, y, z; \lambda, \mu)) d\mu d\lambda. \end{aligned} \quad (4)$$

The form of the displacement function in the pipes was presented in the form proposed in the paper [30]

$$\begin{aligned} \vec{U}_1 = & \sum_{k=1}^3 \int_{-\infty}^{\infty} \sum_{m=-\infty}^{\infty} A_{k,m}^{(1)}(\lambda) \cdot \vec{R}_{k,m}(\rho_1, \varphi_1, z; \lambda) + \tilde{A}_{k,m}^{(1)}(\lambda) \cdot \vec{S}_{k,m}(\rho_1, \varphi_1, z; \lambda) d\lambda, \\ \vec{U}_2 = & \sum_{k=1}^3 \int_{-\infty}^{\infty} \sum_{m=-\infty}^{\infty} A_{k,m}^{(2)}(\lambda) \cdot \vec{R}_{k,m}(\rho_2, \varphi_2, z; \lambda) + \tilde{A}_{k,m}^{(2)}(\lambda) \cdot \vec{S}_{k,m}(\rho_2, \varphi_2, z; \lambda) d\lambda, \end{aligned} \quad (5)$$

where  $H_k(\lambda, \mu)$ ,  $\tilde{H}_k(\lambda, \mu)$ ,  $B_{k,m}^{(p)}(\lambda)$ ,  $A_{k,m}^{(1)}(\lambda)$ ,  $\tilde{A}_{k,m}^{(1)}(\lambda)$ ,  $A_{k,m}^{(2)}(\lambda)$ ,  $\tilde{A}_{k,m}^{(2)}(\lambda)$  are unknown functions that should be found from the boundary conditions (1).

Basic solutions of the Lamé equation Ламе  $\vec{S}_{k,m}(\rho_p, \varphi_p, z; \lambda)$ ,  $\vec{R}_{k,m}(\rho_p, \varphi_p, z; \lambda)$ ,  $\vec{u}_k^{(+)}(x, y, z; \lambda, \mu)$ ,  $\vec{u}_k^{(-)}(x, y, z; \lambda, \mu)$  is presented in the form [18]

$$\begin{aligned} \vec{u}_k^{\pm}(x, y, z; \lambda, \mu) &= N_k^{(d)} e^{i(\lambda z + \mu x) \pm \gamma y}; \\ \vec{R}_{k,m}(\rho, \varphi, z; \lambda) &= N_k^{(p)} I_m(\lambda \rho) e^{i(\lambda z + m\varphi)}; \\ \vec{S}_{k,m}(\rho, \varphi, z; \lambda) &= N_k^{(p)} \left[ (\text{sign } \lambda)^m K_m(|\lambda| \rho) \cdot e^{i(\lambda z + m\varphi)} \right]; \quad k = 1, 2, 3; \end{aligned}$$

$$N_1^{(d)} = \frac{1}{\lambda} \nabla; \quad N_2^{(d)} = \frac{4}{\lambda} (\nu - 1) \vec{e}_2^{(1)} + \frac{1}{\lambda} \nabla(y \cdot); \quad N_3^{(d)} = \frac{i}{\lambda} \text{rot}(\vec{e}_3^{(1)} \cdot); \quad N_1^{(p)} = \frac{1}{\lambda} \nabla;$$

$$N_2^{(p)} = \frac{1}{\lambda} \left[ \nabla \left( \rho \frac{\partial}{\partial \rho} \right) + 4(\nu - 1) \left( \nabla - \vec{e}_3^{(2)} \frac{\partial}{\partial z} \right) \right]; \quad N_3^{(p)} = \frac{i}{\lambda} \text{rot}(\vec{e}_3^{(2)} \cdot); \quad \gamma = \sqrt{\lambda^2 + \mu^2}, \quad -\infty < \lambda, \mu < \infty,$$

where  $\nu$  is the Poisson's ratio;  $I_m(x)$ ,  $K_m(x)$  are modified Bessel functions.

As a result, an infinite system of integro-algebraic equations with 8 unknowns was obtained. Four equations of this system were obtained from the boundary conditions (1) and four more – from the conjugation conditions between the layer and the pipes (2) and (3). The known functions (1) were previously represented through the double Fourier integral for the layer, and for the inner surfaces of the pipes through the Fourier series and integral. After that, the right and left sides of the equations were freed from the Fourier integrals and series. Since the above equations are presented in different coordinate systems, the transition formulas between the basic solutions were used to reduce them to one coordinate system [18]:

– from external solutions for the cylinder  $\vec{S}_{k,m}$  to solutions for the layer  $\vec{u}_k^{(-)}$  (at  $y > 0$ ) and  $\vec{u}_k^{(+)}$  (at  $y < 0$ )

$$\begin{aligned}\bar{S}_{k,m}(\rho_p, \varphi_p, z; \lambda) &= \frac{(-i)^m}{2} \int_{-\infty}^{\infty} \omega_{\mp}^m \cdot e^{-i\mu\bar{x}_p \pm \gamma\bar{y}_p} \cdot \bar{u}_k^{(\mp)} \cdot \frac{d\mu}{\gamma}, \quad k=1, 3; \\ \bar{S}_{2,m}(\rho_p, \varphi_p, z; \lambda) &= \frac{(-i)^m}{2} \int_{-\infty}^{\infty} \omega_{\mp}^m \cdot \left( \left( \pm m \cdot \mu - \frac{\lambda^2}{\gamma} \pm \lambda^2 \bar{y}_p \right) \bar{u}_1^{(\mp)} \mp \lambda^2 \bar{u}_2^{(\mp)} \pm 4\mu(1-\sigma)\bar{u}_3^{(\mp)} \right) \cdot \frac{e^{-i\mu\bar{x}_p \pm \gamma\bar{y}_p} d\mu}{\gamma^2},\end{aligned}\quad (6)$$

where  $\gamma = \sqrt{\lambda^2 + \mu^2}$ ,  $\omega_{\mp}(\lambda, \mu) = \frac{\mu \mp \gamma}{\lambda}$ ,  $m = 0, \pm 1, \pm 2, \dots$ ;

– from the solutions of the layer  $\bar{u}_k^{(+)}$  and  $\bar{u}_k^{(-)}$  to the internal solutions of the cylinder  $\bar{R}_{k,m}$

$$\begin{aligned}\bar{u}_k^{(\pm)}(x, y, z) &= e^{i\mu\bar{x}_p \pm \gamma\bar{y}_p} \cdot \sum_{m=-\infty}^{\infty} (i \cdot \omega_{\mp})^m \bar{R}_{k,m}, \quad (k=1, 3); \\ \bar{u}_2^{(\pm)}(x, y, z) &= e^{i\mu\bar{x}_p \pm \gamma\bar{y}_p} \cdot \sum_{m=-\infty}^{\infty} \left[ (i \cdot \omega_{\mp})^m \cdot \lambda^{-2} \left( (m \cdot \mu + \bar{y}_p \cdot \lambda^2) \cdot \bar{R}_{1,m} \pm \gamma \cdot \bar{R}_{2,m} + 4\mu(1-\sigma)\bar{R}_{3,m} \right) \right],\end{aligned}\quad (7)$$

where  $\bar{R}_{k,m} = \tilde{b}_{k,m}(\rho_p, \lambda) \cdot e^{i(m\varphi_p + \lambda z)}$ ;  $\tilde{b}_{1,n}(\rho, \lambda) = \bar{e}_{\rho} \cdot I'_n(\lambda\rho) + i \cdot I_n(\lambda\rho) \cdot \left( \bar{e}_{\varphi} \frac{n}{\lambda\rho} + \bar{e}_z \right)$ ;

$$\tilde{b}_{2,n}(\rho, \lambda) = \bar{e}_{\rho} \cdot \left[ (4\sigma - 3) \cdot I'_n(\lambda\rho) + \lambda\rho I''_n(\lambda\rho) \right] + \bar{e}_{\varphi} i \cdot m \left( I'_n(\lambda\rho) + \frac{4(\sigma - 1)}{\lambda\rho} I_n(\lambda\rho) \right) + \bar{e}_z i \lambda \rho I'_n(\lambda\rho);$$

$$\tilde{b}_{3,n}(\rho, \lambda) = - \left[ \bar{e}_{\rho} \cdot I_n(\lambda\rho) \frac{n}{\lambda\rho} + \bar{e}_{\varphi} \cdot i \cdot I'_n(\lambda\rho) \right]; \quad \bar{e}_{\rho}, \bar{e}_{\varphi}, \bar{e}_z \text{ are unit vectors in a cylindrical coordinate system;}$$

– from the cylinder solutions with the number  $p$  to the cylinder solutions with the number  $q$

$$\bar{S}_{k,m}(\rho_p, \varphi_p, z; \lambda) = \sum_{n=-\infty}^{\infty} \bar{b}_{k,pq}^{mn}(\rho_q) \cdot e^{i(n\varphi_q + \lambda z)}, \quad k=1, 2, 3;$$

$$\bar{b}_{1,pq}^{mn}(\rho_q) = (-1)^n \tilde{K}_{m-n}(\lambda \ell_{pq}) \cdot e^{i(m-n)\alpha_{pq}} \cdot \tilde{b}_{1,n}(\rho_q, \lambda);$$

$$\bar{b}_{3,pq}^{mn}(\rho_q) = (-1)^n \tilde{K}_{m-n}(\lambda \ell_{pq}) \cdot e^{i(m-n)\alpha_{pq}} \cdot \tilde{b}_{3,n}(\rho_q, \lambda); \quad (8)$$

$$\bar{b}_{2,pq}^{mn}(\rho_q) = (-1)^n \left\{ \tilde{K}_{m-n}(\lambda \ell_{pq}) \cdot \tilde{b}_{2,n}(\rho_q, \lambda) - \frac{\lambda}{2} \ell_{pq} \cdot \left[ \tilde{K}_{m-n+1}(\lambda \ell_{pq}) + \tilde{K}_{m-n-1}(\lambda \ell_{pq}) \right] \cdot \tilde{b}_{1,n}(\rho_q, \lambda) \right\} \cdot e^{i(m-n)\alpha_{pq}},$$

where  $\alpha_{pq}$  is the angle between the axis  $x_p$  and a segment  $\ell_{pq}$ ,  $\tilde{K}_m(x) = (\text{sign}(x))^m \cdot K_m(|x|)$ .

Thus, after using the formulas for the transition of basic solutions between coordinate systems (6)–(8), each equation was written in its local coordinate system. As a result of the transformations, an infinite system of linear algebraic equations of the second kind was obtained, to which the reduction method was applied. Fulfillment of boundary conditions during numerical study showed high accuracy and convergence of results during its solution.

### Numerical studies of the stressed state

The elastic isotropic layer has two thick-walled cylindrical tubes with an outer radius of  $R_1=R_2=16$  mm, internal radius of  $\tilde{R}_1=\tilde{R}_2=11$  mm (Fig. 1). Physical characteristics of the layer: aluminum alloy D16T, Poisson's ratio  $\nu_0=0.3$ , modulus of elasticity  $E_0=7.1 \times 10^4$  MPa. Physical characteristics of pipes: steel SHKH15, Poisson's ratio  $\nu_0=0.28$ , modulus of elasticity  $E_0=2.16 \times 10^5$  MPa. Geometric parameters of the model:  $h=\tilde{h}=32$  mm,  $\alpha_{12}=0$ . The distance between the pipes is chosen in two options:  $l_{12}=50$  mm and  $l_{12}=100$  mm.

At the upper and lower boundaries of the layer, normal stresses are given in the form of a unit wave

$$\sigma_y^{(h)}(x, z) = \sigma_y^{(\tilde{h})}(x, z) = -10^8 \cdot (z^2 + 10^2)^{-2} \cdot \left( \left( x - \frac{\ell_{12}}{2} \right)^2 + 10^2 \right)^{-2} \quad \text{and zero tangential stresses are}$$

$$\tau_{yx}^{(h)} = \tau_{yz}^{(h)} = \tau_{yx}^{(\tilde{h})} = \tau_{yz}^{(\tilde{h})} = 0. \quad \text{Zero stresses are set on the inner surfaces of the pipes } \sigma_\rho^{(p)} = \tau_{\rho\phi}^{(p)} = \tau_{\rho z}^{(p)} = 0.$$

The infinite system was truncated by the parameter  $m=5$  (the number of terms of the Fourier series and the order of the system of equations).

The accuracy of fulfilling the boundary conditions at the specified  $m$  and given geometric parameters is not less than  $10^{-5}$  with values from 0 to 1.

Fig. 2 shows the stresses  $\sigma_\phi$  on the inner surface of the left pipe depending on the distance between the pipes.

Stresses graph  $\sigma_\phi$  (Fig. 2) shows the inverse dependence of the magnitude of the stresses on the distance between the supports, i.e. as the distance between the inclusions decreases, the stresses increase. Also, at angles close to  $\phi=\pi/3$  and  $\phi=2\pi/3$ , on the graphs for the distance between pipes of  $l_{12}=50$  mm, a clearly expressed maximum of positive stresses is observed, which is absent when increasing distance. The maximum stresses are negative at  $\phi=0$  and are equal to  $\sigma_{\phi(\max)}=0.5069$  MPa.

In addition, from the comparisons of the graphs of circumferential stresses (Fig. 2) at  $l_{12}=50$  mm, and at  $l_{12}=100$  mm it is seen that depending on the distance between the pipes not only the values of the stresses change, but also the character of the diagram, and the sign of the stresses can change to the opposite.

Fig. 3 shows the stresses  $\sigma_z$  on the inner surface of the left pipe depending on the distance between the pipes.

Stresses  $\sigma_z$  on the inner surface of the pipe (Fig. 3), as well as stresses  $\sigma_\phi$  (Fig. 2), have an inverse dependence of the stresses magnitude on the distance between the supports. At angles close to  $\phi=\pi/3$ ,  $\phi=2\pi/3$ , and with the distance between the pipes of  $l_{12}=50$  mm clearly maximum stresses  $\sigma_z$  values are observed, which, when increasing distance, decrease significantly, and the maximum stresses shift to  $\phi=0$ .

On the verge of conjugation, stresses  $\sigma_z$  are attenuated.

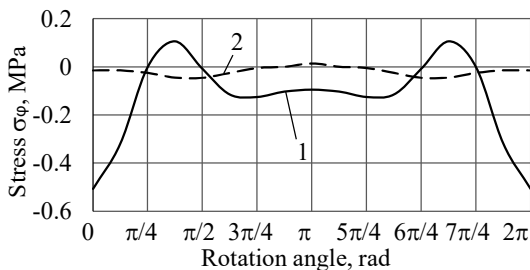


**Fig. 2. Stresses  $\sigma_\phi$  on the inner surface of the pipe:**  
1 – distance  $l_{12}=50$  mm, 2 – distance  $l_{12}=100$  mm

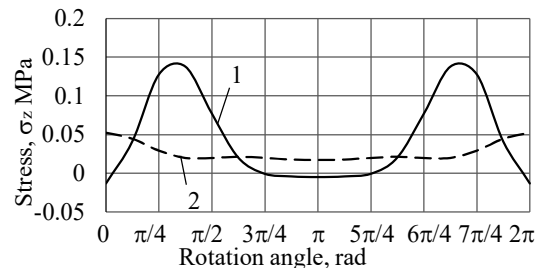


**Fig. 3. Stresses  $\sigma_z$  on the inner surface of the pipe:**  
1 – distance  $l_{12}=50$  mm, 2 – distance  $l_{12}=100$  mm

Fig. 4 shows the stresses  $\sigma_p$  at the conjugation between the pipe ( $p=1$ ) and layer (in the pipe body) depending on the distance between the pipes.

On the inner surface of the pipe, stresses  $\sigma_p$  are set to zero. However, the outer surface of the pipe (the conjugation surface) is compressed and these stresses increase significantly. Compression at the conjugation surface is physically correct because the layer is compressed by loads at the upper and lower boundaries of the layer.

As the distance between the pipes increases, the stresses  $\sigma_p$  at the conjugation surface decrease significantly. The maximum compressive stresses at  $l_{12}=50$  mm are equal to  $\sigma_p = -0.084$  MPa (Fig. 4), at  $l_{12}=100$  mm –  $\sigma_p = -0.013$  MPa.

Stresses  $\sigma_\phi$  at  $l_{12}=50$  mm on the inner and outer surfaces of the pipe  $p=1$  are shown in Fig. 5.

Comparing stresses  $\sigma_\phi$  on the inner and outer surfaces of the pipe (Fig. 5), we can conclude that, unlike the stress  $\sigma_p$ , stresses  $\sigma_\phi$  decrease at the conjugation surface (in the pipe body). Also, these stresses become permanently compressed.

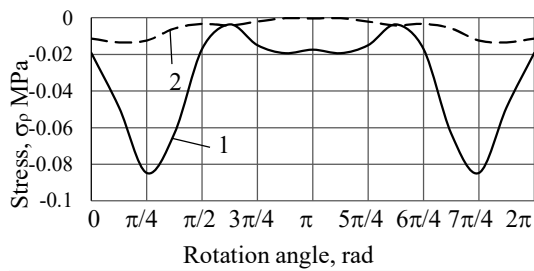


**Fig. 4. Stresses  $\sigma_\phi$  on the outer surface of the pipe:**  
1 – distance  $l_{12}=50$  mm, 2 – distance  $l_{12}=100$  mm

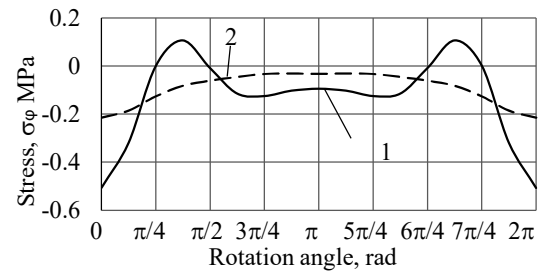


**Fig. 5. Stresses  $\sigma_\phi$ :**  
1 – on the inner surface of the pipe, 2 – on the outer surface

At the conjugation surface (in the pipe body) at  $l_{12}=100$  mm nature of stress  $\sigma_\phi$  distribution remains similar to that shown in Fig. 5, but with smaller values.

## Conclusions

An analytical-numerical method for solving the problem for a layer with two thick-walled pipes at given stresses on the surfaces of the layer and the internal surfaces of the pipes has been created. The problem takes into account the conditions of the conjugation of the layer and pipes - a rigid connection, in which the displacements and stresses along the surface of the connection in the layer are equal, respectively, to the displacements and stresses in the pipes.

For the first time, the solution for a layer with cylindrical pipes has been written in analytical form.

The problem is reduced to an infinite system of linear algebraic equations, which allows the application of the reduction method to it, after which it was solved using the analytical-numerical generalized Fourier method. This made it possible to obtain a solution to the problem with a given accuracy.

A numerical analysis of the stress state with a variation of the distance between the pipes has been performed. Graphs of the distribution of internal stresses in the pipes and the layer have been obtained. The results show an inverse relationship between the magnitude of the stresses and the distance between the pipes: with increasing distance, the magnitude of the stresses decreases. Moreover, in addition to the magnitude, changes in the nature of the diagrams and the sign of the stresses are possible.

The proposed solution method makes it possible to obtain the results of the stress-strain state for most pipes, as well as to evaluate the influence of geometric parameters on the magnitude and distribution of stresses in structures, which can be represented in the form of models similar to the one under consideration.

In the future, when studying the specified topic, it is necessary to consider models where pipes are combined with other types of inhomogeneities (cavities, supports, etc.).

## References

1. Aitharaju, V., Aashat, S., Kia, H., Satyanarayana, A., & Bogert, P. (2016). Progressive damage modeling of notched composites. NASA Technical Reports Server. <https://ntrs.nasa.gov/archive/nasa/casi.ntrs.nasa.gov/20160012242.pdf>.
2. Kondratiev, A. V., Gaidachuk, V. E., & Kharchenko, M. E. (2019). Relationships between the ultimate strengths of polymer composites in static bending, compression, and tension. *Mechanics of Composite Materials*, vol. 55, iss. 2, pp. 259–266. <https://doi.org/10.1007/s11029-019-09808-x>.
3. Tekkaya, A. E. & Soyarslan, C. (2014). Finite element method. In: Laperrière, L., Reinhart, G. (eds) CIRP Encyclopedia of Production Engineering. Berlin, Heidelberg: Springer, pp. 508–514. [https://doi.org/10.1007/978-3-642-20617-7\\_16699](https://doi.org/10.1007/978-3-642-20617-7_16699).
4. Static Structural Simulation Using Ansys Discovery. <https://courses.ansys.com/index.php/courses/structural-simulation>.
5. Zasovenko, A. V. & Fasoliak, A. V. (2023). *Matematychni modeliuvannia dynamiky pruzhnoho pivprostoru z tsylindrychnoiu porozhnynoi, yaka pidkriplena obolonkoiu, pry osesymetrychnykh navantazhenniakh* [Mathematical modeling of the dynamics of an elastic half-medium with a cylindrical cavity reinforced by a shell under axisymmetric loads]. *Novi materialy i tekhnologii v metalurhii ta mashynobuduvanni – New Materials and Technologies in Metallurgy and Mechanical Engineering*, no. 2, pp. 67–73 (in Ukrainian). <https://doi.org/10.15588/1607-6885-2023-2-10>.
6. Guz, A. N., Kubenko, V. D., & Cherevko, M. A. (1978). *Difraktsiya uprugikh voln* [Elastic wave diffraction]. Kyiv: Naukova dumka, 307 p. (in Russian).



7. Grinchenko, V. T. & Meleshko, V. V. (1981). *Garmonicheskiye kolebaniya i volny v uprugikh telakh* [Harmonic vibrations and waves in elastic bodies]. Kyiv: Naukova dumka, 284 p. (in Russian).
8. Smetankina, N., Kurenov, S., & Barakhov, K. (2023). Dynamic stresses in the adhesive joint. The Goland-Reissner model. In: Cioboată D. D. (eds) *International Conference on Reliable Systems Engineering (ICoRSE) – 2023. ICoRSE 2023. Lecture Notes in Networks and Systems*. Cham: Springer, vol. 762, pp. 456–468. [https://doi.org/10.1007/978-3-031-40628-7\\_38](https://doi.org/10.1007/978-3-031-40628-7_38).
9. Ugrimov, S., Smetankina, N., Kravchenko, O., Yareshchenko, V., & Kruszka, L. (2023). A study of the dynamic response of materials and multilayer structures to shock loads. In: Altenbach H., et al. *Advances in Mechanical and Power Engineering. CAMPE 2021. Lecture Notes in Mechanical Engineering*. Cham: Springer, pp. 304–313. [https://doi.org/10.1007/978-3-031-18487-1\\_31](https://doi.org/10.1007/978-3-031-18487-1_31).
10. Smetankina, N., Merkulova, A., Merkulov, D., Misura, S., & Misiura, Ie. (2023). Modelling thermal stresses in laminated aircraft elements of a complex form with account of heat sources. In: Cioboată D. D. (eds) *International Conference on Reliable Systems Engineering (ICoRSE) – 2022. ICoRSE 2022. Lecture Notes in Networks and Systems*. Cham: Springer, vol. 534, pp. 233–246. [https://doi.org/10.1007/978-3-031-15944-2\\_22](https://doi.org/10.1007/978-3-031-15944-2_22).
11. Smetankina, N., Kravchenko, I., Merkulov, V., Ivchenko, D., & Malykhina, A. (2020). Modelling of bird strike on an aircraft glazing. In book: Nechyporuk M., Pavlikov V., Kritskiy D. (eds) *Integrated Computer Technologies in Mechanical Engineering. Advances in Intelligent Systems and Computing*. Cham: Springer, vol. 1113, pp. 289–297. [https://doi.org/10.1007/978-3-030-37618-5\\_25](https://doi.org/10.1007/978-3-030-37618-5_25).
12. Fesenko, A. & Vaysfel'd, N. (2019). The wave field of a layer with a cylindrical cavity. In: Gdoutos, E. (eds) *Proceedings of the Second International Conference on Theoretical, Applied and Experimental Mechanics. ICTAEM 2019. Structural Integrity*, vol. 8. Cham: Springer, pp. 277–282. [https://doi.org/10.1007/978-3-030-21894-2\\_51](https://doi.org/10.1007/978-3-030-21894-2_51).
13. Fesenko, A. & Vaysfel'd, N. (2021). The dynamical problem for the infinite elastic layer with a cylindrical cavity. *Procedia Structural Integrity*, vol. 33, pp. 509–527. <https://doi.org/10.1016/j.prostr.2021.10.058>.
14. Jafari, M., Chaleshtari, M. H. B., Khoramishad, H., & Altenbach H. (2022). Minimization of thermal stress in perforated composite plate using metaheuristic algorithms WOA, SCA and GA. *Composite Structures*, vol. 304, part 2, article 116403. <https://doi.org/10.1016/j.compstruct.2022.116403>.
15. Malits, P. (2021). Torsion of an elastic half-space with a cylindrical cavity by a punch. *European Journal of Mechanics – A/Solids*, vol. 89, article 104308. <https://doi.org/10.1016/j.euromechsol.2021.104308>.
16. Khechai, A., Belarbi, M.-O., Bouaziz, A., & Rebbi, F. M. L. (2023). A general analytical solution of stresses around circular holes in functionally graded plates under various in-plane loading conditions. *Acta Mechanica*, vol. 234, pp. 671–691. <https://doi.org/10.1007/s00707-022-03413-1>.
17. Snitser, A. R. (1996). The reissner-sagoci problem for a multilayer base with a cylindrical cavity. *Journal of Mathematical Sciences*, vol. 82, iss. 3, pp. 3439–3443. <https://doi.org/10.1007/bf02362661>.
18. Nikolayev, A. G. & Protsenko, V. S. (2011). *Obobshchennyi metod Fur'ye v prostranstvennykh zadachakh teorii uprugosti* [Generalized Fourier method in spatial problems of the theory of elasticity]. Kharkiv: National Aerospace University "Kharkiv Aviation Institute", 344 p. (in Russian).
19. Nikolaev, A. G. & Tanchik, E. A. (2015). The first boundary-value problem of the elasticity theory for a cylinder with N cylindrical cavities. *Numerical Analysis and Applications*, vol. 8, pp. 148–158. <https://doi.org/10.1134/S1995423915020068>.
20. Nikolaev, A. G. & Tanchik, E. A. (2016). Stresses in an elastic cylinder with cylindrical cavities forming a hexagonal structure. *Journal of Applied Mechanics and Technical Physics*, vol. 57, pp. 1141–1149. <https://doi.org/10.1134/S0021894416060237>.
21. Nikolaev, A. G. & Tanchik, E. A. (2016). Model of the stress state of a unidirectional composite with cylindrical fibers forming a tetragonal structure. *Mechanics of Composite Materials*, vol. 52, pp. 177–188. <https://doi.org/10.1007/s11029-016-9571-6>.
22. Nikolayev, A. G. & Orlov, Ye. M. (2012). *Resheniye pervoy osesimmetrichnoy termouprugoy krayevoy zadachi dlya transversalno-izotropnogo poluprostranstva so sferoidalnoy polostyu* [Solution of the first axisymmetric thermoelastic boundary value problem for a transversally isotropic half-space with a spheroidal cavity]. *Problemy vychislitel'noy mekhaniki i prochnosti konstruksiy – Problems of Computational Mechanics and Strength of Structures*, iss. 20, pp. 253–259 (in Russian).
23. Ukrayinets, N., Murahovska, O., & Prokhorova, O. (2021). Solving a one mixed problem in elasticity theory for half-space with a cylindrical cavity by the generalized Fourier method. *Eastern-European Journal of Enterprise Technologies*, vol. 2, no. 7 (110), pp. 48–57. <https://doi.org/10.15587/1729-4061.2021.229428>.
24. Miroshnikov, V. Yu., Denysova, T. V., & Protsenko, V. S. (2019). *Doslidzhennia pershoi osnovnoi zadachi teorii pruzhnosti dlia sharu z tsylindrychnoiu porozhnynoiu* [Study of the first fundamental problem of the theory of elasticity for a layer with a cylindrical cavity]. *Opir materialiv i teoriia sporud – Strength of Materials and Theory of Structures*, no. 103, pp. 208–218 (in Ukrainian). <https://doi.org/10.32347/2410-2547.2019.103.208-218>.



25. Miroshnikov, V. Yu., Medvedeva, A. V., & Oleshkevich, S. V. (2019). Determination of the stress state of the layer with a cylindrical elastic inclusion. *Materials Science Forum*, vol. 968, pp. 413–420. <https://doi.org/10.4028/www.scientific.net/MSF.968.413>.
26. Miroshnikov, V. Yu. (2019). Investigation of the stress state of a composite in the form of a layer and a half space with a longitudinal cylindrical cavity at stresses given on boundary surfaces. *Journal of Mechanical Engineering – Problemy Mashynobuduvannia*, vol. 22, no. 4, pp. 24–31. <https://doi.org/10.15407/pmach2019.04.024>.
27. Miroshnikov, V. Yu., Savin, O. B., Hrebennikov, M. M., & Demenko, V. F. (2023). Analysis of the stress state for a layer with two incut cylindrical supports. *Journal of Mechanical Engineering – Problemy Mashynobuduvannia*, vol. 26, no. 1, pp. 15–22. <https://doi.org/10.15407/pmach2023.01.015>.
28. Miroshnikov, V. Yu., Savin, O. B., Hrebennikov, M. M., & Pohrebniak, O. A. (2022). Analysis of the stress state of a layer with two cylindrical elastic inclusions and mixed boundary conditions. *Journal of Mechanical Engineering – Problemy Mashynobuduvannia*, vol. 25, no. 2, pp. 22–29. <https://doi.org/10.15407/pmach2022.02.022>.
29. Miroshnikov, V. Yu. (2019). Investigation of the stress strain state of the layer with a longitudinal cylindrical thick-walled tube and the displacements given at the boundaries of the layer. *Journal of Mechanical Engineering – Problemy Mashynobuduvannia*, vol. 22, no. 2, pp. 44–52. <https://doi.org/10.15407/pmach2019.02.044>.
30. Miroshnikov, V. (2023). Rotation of the layer with the cylindrical pipe around the rigid cylinder. In: Altenbach H., et al. *Advances in Mechanical and Power Engineering. CAMPE 2021. Lecture Notes in Mechanical Engineering*. Cham: Springer, pp. 314–322. [https://doi.org/10.1007/978-3-031-18487-1\\_32](https://doi.org/10.1007/978-3-031-18487-1_32).

*Received 31 May 2024*

## **Перша основна задача теорії пружності для шару композиту з двома товстостінними трубами**

**О. Ю. Деньщиков, В. П. Пелих, Я. В. Гребенюк, В. Ю. Мірошніков**

Національний аерокосмічний університет ім. М. Є. Жуковського «Харківський авіаційний інститут»,  
61070, Україна, м. Харків, вул. Вадима Манька, 17

*Розв'язана просторова задача теорії пружності для волокнистого композиту у вигляді шару з двома циліндричними товстостінними трубами. На плоских поверхнях шару й на внутрішній поверхні труб задані напруження. Задача представлена у вигляді розв'язків рівнянь Ламе в різних системах координат, де шар розглядається в декартовій системі, труби – у локальних циліндричних. Для поєднання базисних розв'язків у різних системах координат застосовується узагальнений метод Фур'є. Задовольняючи граничним умовам і умовам спряження між шаром і трубами, формується нескінчена система інтегро-алгебраїчних рівнянь, які зводяться до лінійних алгебраїчних рівнянь другого роду і використовується метод редукції. Після знаходження невідомих можна отримати напружено-деформований стан у будь-якій точці пружних поєднаних тіл. Задля цього до базисних розв'язків задачі також застосовується узагальнений метод Фур'є. По результатах чисельних досліджень можемо стверджувати, що задачу можна розв'язати із заданою точністю, яка залежить від порядку системи рівнянь. Числовий аналіз напруженого стану розглянуто з варіацією відстані між трубами. Отримані графіки розподілення внутрішніх напружень у трубах і шарі. Результати показують зворотну залежність між величиною напружень і відстанню між трубами. Крім абсолютної величини напружень, можливі зміни в характері епюр і знаку. Запропонований метод розв'язання може бути використаний під час проектування деталей і механізмів, розрахункова модель яких представляє собою шар із циліндричними трубами, в машино- й авіабудуванні. Отриманий напружено-деформований стан дає змогу попередньої оцінки геометричні параметри конструкції. Подальший розгляд теми дослідження необхідний для моделі, де труби комбінуються з іншими типами неоднорідностей.*

**Ключові слова:** волокнистий композит, узагальнений метод Фур'є, рівняння Ламе.

### **Література**

1. Aitharaju V., Aashat S., Kia H., Satyanarayana A., Bogert P. Progressive damage modeling of notched composites. NASA Technical Reports Server. 2016. <https://ntrs.nasa.gov/archive/nasa/casi.ntrs.nasa.gov/20160012242.pdf>.
2. Kondratiev A. V., Gaidachuk V. E., Kharchenko M. E. Relationships between the ultimate strengths of polymer composites in static bending, compression, and tension. *Mechanics of Composite Materials*. 2019. Vol. 55. Iss. 2. P. 259–266. <https://doi.org/10.1007/s11029-019-09808-x>.
3. Tekkaya A. E., Soyarslan C. Finite element method. In: Laperrière L., Reinhart G. (eds) *CIRP Encyclopedia of Production Engineering*. Berlin, Heidelberg: Springer, 2014. P. 508–514. [https://doi.org/10.1007/978-3-642-20617-7\\_16699](https://doi.org/10.1007/978-3-642-20617-7_16699).

4. Static Structural Simulation Using Ansys Discovery. <https://courses.ansys.com/index.php/courses/structural-simulation>.
5. Засовенко А. В., Фасоляк А. В. Математичне моделювання динаміки пружного півпростору з циліндричною порожниною, яка підкріплена оболонкою, при осесиметричних навантаженнях. *Нові матеріали і технології в металургії та машинобудуванні*. 2023. № 2. С. 67–73. <https://doi.org/10.15588/1607-6885-2023-2-10>.
6. Гузь А. Н., Кубенко В. Д., Черевко М. А. Дифракція упругих волн. Київ: Наукова думка, 1978. 307 с.
7. Гринченко В. Т., Мелешко В. В. Гармонические колебания и волны в упругих телах. Київ: Наукова думка, 1981. 284 с.
8. Smetankina N., Kurennov S., Barakhov K. Dynamic stresses in the adhesive joint. The Goland-Reissner model. In: Cioboată D. D. (eds) *International Conference on Reliable Systems Engineering (ICoRSE) – 2023. ICoRSE 2023. Lecture Notes in Networks and Systems*. Cham: Springer, 2023. Vol. 762. P. 456–468. [https://doi.org/10.1007/978-3-031-40628-7\\_38](https://doi.org/10.1007/978-3-031-40628-7_38).
9. Ugrimov S., Smetankina N., Kravchenko O., Yareshchenko V., Kruszka L. A study of the dynamic response of materials and multilayer structures to shock loads. In: Altenbach H., et al. *Advances in Mechanical and Power Engineering. CAMPE 2021. Lecture Notes in Mechanical Engineering*. Cham: Springer, 2023. P. 304–313. [https://doi.org/10.1007/978-3-031-18487-1\\_31](https://doi.org/10.1007/978-3-031-18487-1_31).
10. Smetankina N., Merkulova A., Merkulov D., Misura S., Misiura Ie. Modelling thermal stresses in laminated aircraft elements of a complex form with account of heat sources. In: Cioboată D. D. (eds) *International Conference on Reliable Systems Engineering (ICoRSE) – 2022. ICoRSE 2022. Lecture Notes in Networks and Systems*. Cham: Springer, 2023. Vol. 534. P. 233–246. [https://doi.org/10.1007/978-3-031-15944-2\\_22](https://doi.org/10.1007/978-3-031-15944-2_22).
11. Smetankina N., Kravchenko I., Merkulov V., Ivchenko D., Malykhina A. Modelling of bird strike on an aircraft glazing. In book: Nechyporuk M., Pavlikov V., Kritskiy D. (eds) *Integrated Computer Technologies in Mechanical Engineering. Advances in Intelligent Systems and Computing*. Cham: Springer, 2020. Vol. 1113. P. 289–297. [https://doi.org/10.1007/978-3-030-37618-5\\_25](https://doi.org/10.1007/978-3-030-37618-5_25).
12. Fesenko A., Vaysfel'd N. The wave field of a layer with a cylindrical cavity. In: Gdoutos, E. (eds) *Proceedings of the Second International Conference on Theoretical, Applied and Experimental Mechanics. ICTAEM 2019. Structural Integrity*. Cham: Springer, 2019. Vol. 8. P. 277–282. [https://doi.org/10.1007/978-3-030-21894-2\\_51](https://doi.org/10.1007/978-3-030-21894-2_51).
13. Fesenko A., Vaysfel'd N. The dynamical problem for the infinite elastic layer with a cylindrical cavity. *Procedia Structural Integrity*. 2021. Vol. 33. P. 509–527. <https://doi.org/10.1016/j.prostr.2021.10.058>.
14. Jafari M., Chaleshtari M. H. B., Khoramishad H., Altenbach H. Minimization of thermal stress in perforated composite plate using metaheuristic algorithms WOA, SCA and GA. *Composite Structures*. 2022. Vol. 304. Part 2. Article 116403. <https://doi.org/10.1016/j.compstruct.2022.116403>.
15. Malits P. Torsion of an elastic half-space with a cylindrical cavity by a punch. *European Journal of Mechanics – A/Solids*. 2021. Vol. 89. Article 104308. <https://doi.org/10.1016/j.euromechsol.2021.104308>.
16. Khechai A., Belarbi M.-O., Bouaziz A., Rebbi F. M. L. A general analytical solution of stresses around circular holes in functionally graded plates under various in-plane loading conditions. *Acta Mechanica*. 2023. Vol. 234. P. 671–691. <https://doi.org/10.1007/s00707-022-03413-1>.
17. Snitser A. R. The reissner-sagoci problem for a multilayer base with a cylindrical cavity. *Journal of Mathematical Sciences*. 1996. Vol. 82. Iss. 3. P. 3439–3443. <https://doi.org/10.1007/bf02362661>.
18. Николаев А. Г., Проценко В. С. Обобщенный метод Фурье в пространственных задачах теории упругости. Харьков: Нац. аэрокосм. ун-т им. Н. Е. Жуковского «ХАИ», 2011. 344 с.
19. Nikolaev A. G., Tanchik E. A. The first boundary-value problem of the elasticity theory for a cylinder with N cylindrical cavities. *Numerical Analysis and Applications*. 2015. Vol. 8. P. 148–158. <https://doi.org/10.1134/S1995423915020068>.
20. Nikolaev A. G., Tanchik E. A. Stresses in an elastic cylinder with cylindrical cavities forming a hexagonal structure. *Journal of Applied Mechanics and Technical Physics*. 2016. Vol. 57. P. 1141–1149. <https://doi.org/10.1134/S0021894416060237>.
21. Nikolaev A. G., Tanchik E. A. Model of the stress state of a unidirectional composite with cylindrical fibers forming a tetragonal structure. *Mechanics of Composite Materials*. 2016. Vol. 52. P. 177–188. <https://doi.org/10.1007/s11029-016-9571-6>.
22. Николаев А. Г., Орлов Е. М. Решение первой осесимметричной термоупругой краевой задачи для трансверсально-изотропного полупространства со сфероидальной полостью. *Проблемы вычислительной механики и прочности конструкций*. 2012. Вып. 20. С. 253–259.
23. Ukrainets N., Murahovska O., Prokhorova O. Solving a one mixed problem in elasticity theory for half-space with a cylindrical cavity by the generalized Fourier method. *Eastern-European Journal of Enterprise Technologies*. 2021. Vol. 2. No. 7 (110). P. 48–57. <https://doi.org/10.15587/1729-4061.2021.229428>.

24. Мірошніков В. Ю., Денисова Т. В., Проценко В. С. Дослідження першої основної задачі теорії пружності для шару з циліндричною порожниною. *Опір матеріалів і теорія споруд*. 2019. № 103. С. 208–218. <https://doi.org/10.32347/2410-2547.2019.103.208-218>.
25. Miroshnikov V. Yu., Medvedeva A. V., Oleshkevich S. V. Determination of the stress state of the layer with a cylindrical elastic inclusion. *Materials Science Forum*. 2019. Vol. 968. P. 413–420. <https://doi.org/10.4028/www.scientific.net/MSF.968.413>.
26. Miroshnikov V. Yu. Investigation of the stress state of a composite in the form of a layer and a half space with a longitudinal cylindrical cavity at stresses given on boundary surfaces. *Journal of Mechanical Engineering – Problemy Mashynobuduvannia*. 2019. Vol. 22. No. 4. P. 24–31. <https://doi.org/10.15407/pmach2019.04.024>.
27. Miroshnikov V. Yu., Savin O. B., Hrebennikov M. M., Demenko V. F. Analysis of the stress state for a layer with two incut cylindrical supports. *Journal of Mechanical Engineering – Problemy Mashynobuduvannia*. 2023. Vol. 26. No. 1. P. 15–22. <https://doi.org/10.15407/pmach2023.01.015>.
28. Miroshnikov V. Yu., Savin O. B., Hrebennikov M. M., Pohrebniak O. A. Analysis of the stress state of a layer with two cylindrical elastic inclusions and mixed boundary conditions. *Journal of Mechanical Engineering – Problemy Mashynobuduvannia*. 2022. Vol. 25. No. 2. P. 22–29. <https://doi.org/10.15407/pmach2022.02.022>.
29. Miroshnikov V. Yu. Investigation of the stress strain state of the layer with a longitudinal cylindrical thick-walled tube and the displacements given at the boundaries of the layer. *Journal of Mechanical Engineering – Problemy Mashynobuduvannia*. 2019. Vol. 22. No. 2. P. 44–52. <https://doi.org/10.15407/pmach2019.02.044>.
30. Miroshnikov V. Rotation of the layer with the cylindrical pipe around the rigid cylinder. In: Altenbach H., et al. *Advances in Mechanical and Power Engineering. CAMPE 2021. Lecture Notes in Mechanical Engineering*. Cham: Springer, 2023. P. 314–322. [https://doi.org/10.1007/978-3-031-18487-1\\_32](https://doi.org/10.1007/978-3-031-18487-1_32).